Arabian Journal of Chemistry (2015) **8**, 293–306

King Saud University

Arabian Journal of Chemistry

www.ksu.edu.sa
www.sciencedirect.com

ORIGINAL ARTICLE

Dioxomolybdenum(VI) chelates of bioinorganic, catalytic, and medicinal relevance: Studies on some *cis*-dioxomolybdenum(VI) complexes involving O, N-donor 4-oximino-2-pyrazoline-5-one derivatives

R.C. Maurya *, J. Chourasia, M.H. Martin, S. Roy, A.K. Sharma, P. Vishwakarma

Coordination and Bioinorganic Chemistry Laboratory, Department of P.G. Studies and Research in Chemistry, R.D. University, Jabalpur 482 001, India

Received 4 November 2010; accepted 12 January 2011
Available online 18 January 2011

KEYWORDS

Dioxomolybdenum(VI) chelates;
O, N-donor oximes;
3D Molecular modeling

Abstract A new series of five mixed-ligand complexes of dioxomolybdenum(VI) of the general composition $[MoO_2(L)_2(H_2O)_2]$, where LH = 4-acetyloxime-3-methyl-1-phenyl-2-pyrazolin-5-one (aomppH), 3-methyl-1-phenyl-4-propionyloxime-2-pyrazolin-5-one (mppopH), 4-butyryloxime-3-methyl-1-phenyl-2-pyrazolin-5-one (buomppH), 4-iso-butyryloxime-3-methyl-1-phenyl-2-pyrazolin-5-one (ibuomppH) or 4-benzoyloxime-3-methyl-1-phenyl-2-pyrazolin-5-one (bomppH) has been synthesized by the interaction of $[MoO_2(acac)_2]$ with the said ligands in ethanol medium. The complexes so obtained were characterized by elemental analyses, molar conductance, decomposition temperature and magnetic measurements, thermogravimetric analyses, ^{1}H NMR, IR, mass, and electronic spectral studies. The 3D molecular modeling and analysis for bond lengths and bond angles have also been carried out for one of the representative compound, $[MoO_2(aomppH)_2(H_2O)_2]$ (**1**) to substantiate the proposed structure.

1. Introduction

Oxime/oximate metal complexes have been investigated actively since the beginning of the last century of the last millennium (Kukushkin and Pombeiro, 1999). Dimethylglyoxime (or diacetyldioxime) was the first organic reagent to be used in analytical chemistry for the estimation of nickel (Tschugaeft, 1905, 1908). Since then, the analytical application of a number of bidentate chelate ligands like dioximes and aromatic hydroxyl aldoximes have been extensively studied (Diehl, 1940; Banks, 1963). Apart from analytical applications, studies have been conducted on their stability data with a variety of metal

* Corresponding author. Tel.: +91 761 2601303; fax: +91 761 2603752.
E-mail address: rcmaurya1@gmail.com (R.C. Maurya).
Peer review under responsibility of King Saud University.

Production and hosting by Elsevier

1878-5352 © 2011 Production and hosting by Elsevier B.V. on behalf of King Saud University.
http://dx.doi.org/10.1016/j.arabjc.2011.01.010

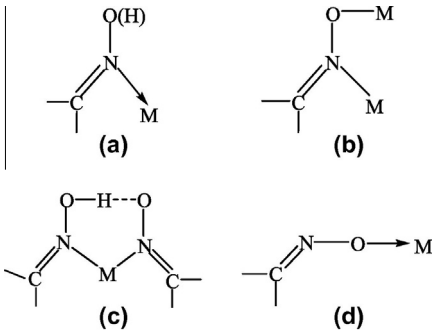

Figure 1 Various coordination modes of oximes.

ions in aqueous medium and also on their coordination behavior (Mehrotra et al., 1975; Singh et al., 1974). Although, oximes are widely recognized as versatile ligands and their complexes with various transition metals have been studied in detail (Mehrotra et al., 1975; Singh et al., 1974), much remains to understand the type of structures that are formed. In general the oxime function is known (Chakravorty, 1974) to coordinate in four ways as shown in Fig. 1. Coordination modes (**a**) and (**c**) are observed most frequently although the oxime group is a poor donor unless it is a part of the chelate ring. Oximes can react either as such or in the form of a conjugate base. This is what is meant by putting the hydrogen atom in (**a**) in parenthesis. This atom may or may not be present. In (**c**) one oxime group is present as such while the second group is present as the conjugate base; the single hydrogen atom is then shared in the O–H···O bridge.

The chelating behavior of 4-oximino-2-pyrazoline-5-ones (Shah and Shah, 1981, 1982a,b; Patel and Shah, 1985; Maurya et al., 2003d; Masoud et al., 1986) is well established. They coordinate through the cyclic carbonyl oxygen and oximino nitrogen, thus behaving as bidentate O, N donors. Since the increasing use of coordination compounds in analytical chemistry, pigments, medicine and biochemistry, many investigators have studied these topics, especially the important role of oxime complexes in chemistry (Pande, 1966; Schrazer, 1976; Brown, 1973; Gok and Bekaroglu, 1981; Irez and Bekaroglu, 1983; Gul and Bekaroglu, 1982; Kocak and Bekaroglu, 1985; Ozcan and Mirzaoglu, 1988; Ucan and Mirzaoglu, 1990; Sevindir and Mirzaoglu, 1992; Karatas et al., 1991a; Ucan and Karatas, 1991; Pekacar and Ozcan, 1994, 1995a,b; Mercimek et al., 1995; Karatas and Ucan, 1998; Karatas et al., 1991b; Reddy et al., 2000; Alexandrova et al., 2000; Yildim et al., 2003; Zulfikaroglu et al., 2003).

The coordination compounds of molybdenum can catalyze a variety of industrially important chemical reactions such as olefin epoxidation (Abrantes et al., 2003; Li et al., 2010), isomerization of allyl alcohols (Franczek et al., 2002), and olefin metathesis (Schrock, 2004). The useful role of molybdenum is not restricted to artificial catalysis alone, since it is an essential element in diverse biological systems, as nature has made use of the molybdenum center in various redox enzymes (Collision et al., 1996; Hille, 1996; Enemark et al., 2004). Oxidized forms of these molybdoenzymes, e.g., aldehyde and sulfite oxidases are supposed to contain *cis*-MoX_2 units (X = O, S) coordinated to sulfur, nitrogen and oxygen donor atoms of the protein structure.

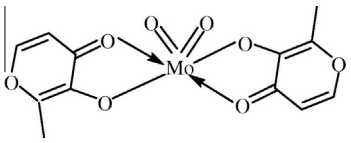

Figure 2 Structure of BMDOM.

The presence of the *cis*-dioxomolybdenum(VI) cation, $[MoO_2]^{+2}$, in the oxidized form of certain molybdoenzymes (Stiefel, 1979a), has stimulated both the search for new structures in which this moiety is coordinated to ligands containing nitrogen, oxygen and/or sulfur donors and also to the study of their chemicals, spectroscopic, and structural properties (Stiefel, 1979b).

Molybdenum bears some resemblance to vanadium. Both vanadate and molybdate can strongly inhibit protein tyrosine phosphatase activity, thus maintaining tyrosine phosphorylation in protein extracts, although molybdate is less strongly bound in the enzyme active site (Elberg et al., 1995). Molybdate was shown to inactivate glycogen synthase and increase the glycolytic flux in rat hepatocytes (Fillat et al., 1992) and to display synergistic stimulation of glucose uptake in rat adipocytes in the presence of H_2O_2 (Elberg et al., 1995; Goto et al., 1992), again analogous to *in vitro* effects of vanadate. Sodium molybdate dihydrate ($Na_2MoO_4{\cdot}2H_2O$), 0.4–0.5 g L^{-1} in drinking water and 0.75–1.25 g Kg^{-1} in food for 8 weeks in STZ-diabetic rats, led to 75% blood glucose lowering and also normalized plasma triglyceride and non-esterified fatty acid levels, without affecting plasma insulin (Ozcelikay et al., 1996), in STZ-diabetic rats. Thus, in view of these findings efforts are being made to synthesize complexes of MoO_2^{2+} containing oxygen and/or nitrogen environment, such as, bis(maltolato)dioxomolybdenum(VI) (BMDOM) complex, $[MoO_2(ma)_2]$ (Shuter, 1995, Fig. 2).

Most molybdenum(VI) complexes contain *cis*-MoO_2^{2+} and an octahedral geometry. Although many precursors are available, $[MoO_2(acac)_2]$ is a convenient source of MoO_2^{2+} (Mohanty and Dash, 1990; Syamal and Maurya, 1989).

In continuation of interest in the synthesis and characterization of coordination compounds of bioinorganic and medicinal relevance, a study was undertaken of the coordination chemistry of dioxomolybdenum(VI) complexes involving 4-oximino-2-pyrazoline-5-ones, such as, 4-acetyloxime-3-methyl-1-phenyl-2-pyrazoline-5-one (aomppH, I), 3-methyl-1-phenyl-4-propionyloxime-2-pyrazoline-5-one (mppopH, II), 4-butyryloxime-3-methyl-1-phenyl-2-pyrazoline-5-one (buomppH, III), 4-isobutyryloxime-3-methyl-1-phenyl-2-pyrazoline-5-one (ibuomppH, IV), 4-benzoyloxime-3-methyl-1-phenyl-2-pyrazoline-5-one (bomppH, V). The structure of the oxime derivatives used in the present study is shown in Fig. 3.

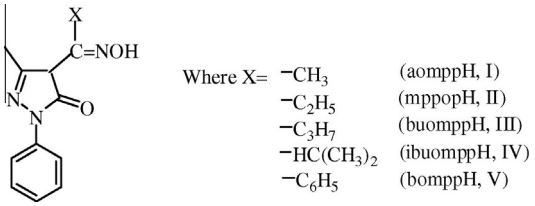

Figure 3 Structures of various oximes.

2. Experimental

2.1. Materials

3-Methyl-1-phenyl-2-pyrazolin-5-one- (Lancaster, UK), benzoyl chloride, acetyl chloride and propionyl chloride, hydroxylamine hydrochloride, acetylacetone, calcium hydroxide (Thomas Baker Chemicals Limited, Mumbai), butyryl chloride, iso-butyryl chloride (Merck, Germany) and Sodium hydroxide (E. Merck India Limited, Mumbai), ammonium molybdate tetrahydrate (Sisco Chem. Industries, Mumbai) were used as supplied. Alcohol was purchased from Bengal Chemicals and Pharmaceuticals Limited, Kolkata. All other chemicals used were of analytical reagent grade.

2.2. Preparation of parent compound

The parent compound bis(acetylacetonato)dioxomolybdenum(VI), $[MoO_2(acac)_2]$ was prepared by the method of Chen et al. (Chen et al., 1976).

2.3. Preparation of different 4-acyl-3-methyl-1-phenyl-2-pyrazolin-5-one

They were prepared by the Jensen's (Jensen, 1959) method with slight modification. Into a one liter 3-necked quick fit flask containing DMF (100 mL) and carrying a dropping funnel, a mechanical stirrer, and a reflux condenser, was placed 3-methyl-1-phenyl-2-pyrazolin-5-one (17 g, 0.098 M). A solution was obtained by gentle heating, and benzoyl chloride (12 mL)/acetyl chloride (5.4 mL)/propionyl chloride 8.94 mL)/butyryl chloride (10.33 mL)/isobutyryl chloride (11 mL) was added drop wise within 2–3 min. The reaction was exothermic and the reaction mixtures became a paste. The mixture was allowed to cool and then refluxed with stirring for 1 h on a sand bath, during which period the bright yellow complex formed initially turned yellowish brown. The complex was decomposed by pouring the reaction mixture into chilled dilute hydrochloric acid solution (500 mL, 3 N). A yellowish brown solid settled, which was filtered in a sintered glass crucible, washed with distilled water until the washings were colorless, and dried in air and recrystallized from *n*-heptane. Some important physical properties are given in the Table 1.

The reaction scheme related to the synthesis of 4-acyl-3-methyl-1-phenyl-2-pyrazolin-5-one is as follows (Scheme 1.).

Table 1 Some physical properties of 4-acyl-3-methyl-1-phenyl-2-pyrazolin-5-one derivatives.

Abbreviation	Empirical formula	m.p.	Color	Yield (%)
bmppH	$(C_{17}H_{14}N_2O_2)$ (278)	90	Yellow	75
bumppH	$(C_{14}H_{16}N_2O_2)$ (244)	65	Yellow	70
amppH	$(C_{12}H_{12}N_2O_2)$ (216)	60	Yellow	50
pmppH	$(C_{13}H_{14}N_2O_2)$ (230)	68	Yellow	60
iso-bumppH	$(C_{14}H_{16}N_2O_2)$ (244)	57	Yellow	50

bmppH = 4-benzoyl-3-methyl-1-phenyl-2-pyrazolin-5-one.
bumppH = 4-butyryl-3-methyl-1-phenyl-2-pyrazolin-5-one.
amppH = 4-acetyl-3-methyl-1-phenyl-2-pyrazolin-5-one.
pmppH = 3-methyl-1-phenyl-4-propionyl-2-pyrazolin-5-one.
Iso-bumppH = 4-*iso*-butyryl-3-methyl-1-phenyl-2-pyrazolin-5-one.

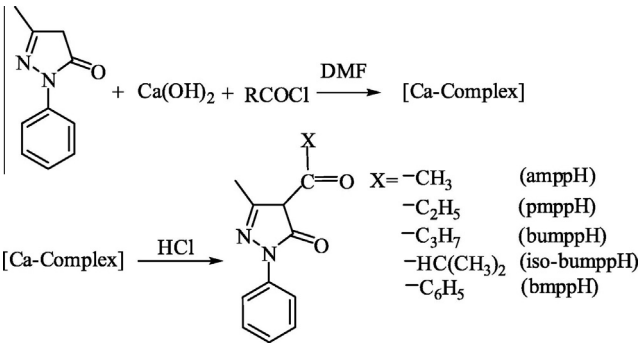

Scheme 1 Reaction scheme for the synthesis of 4-acyl-3-mthyl-1-phenyl-2-pyrazolin-5-one derivatives.

2.4. Preparation of oxime derivatives of bmppH, bumppH, amppH, pmppH, iso-bumppH

These oximes were prepared by following the general method given below: A solution of hydroxylamine hydrochloride (0.347 g, 5 mmol) and sodium hydroxide (0.20 g, 5 mmol) in 40 mL aqueous/ethanol (1:1) was added to a solution of 4-benzoyl-3-methyl-1-phenyl-2-pyrazolin-5-one (1.39 g, 5 mmol), 4-acetyl-3-methyl-1-phenyl-2-pyrazolin-5-one (1.08 g, 5 mmol), 3-methyl-1-phenyl-4-propionyl-2-pyrazolin-5-one (1.15 g, 5 mmol), 4-butyryl-3-methyl-1-phenyl-2-pyrazoline-5-one (1.22 g, 5 mmol), or 4-*iso*-butyryl-3-methyl-1-phenyl-2-pyrazolin-5-one (1.22 g, 5 mmol) in 20 mL ethanol. The mixture was refluxed for two hours. On cooling a crystalline product was obtained, which was filtered by suction, washed several times with water and finally with ethanol. The oxime of 4-benzoyl-3-methyl-1-phenyl-2-pyrazolin-5-one was precipitated by pouring the reaction mixture in excess (150 mL) of distilled water. The characterization data of the oxime derivatives are given in Table 2.

2.5. Preparation of complexes

The oximes derivative, bomppH (0.586 g, 2 mmol), aomppH (0.462 g, 2 mmol), mppopH (0.490 g, 2 mmol), buomppH (0.518 g, 2 mmol) or ibuomppH (0.518 g, 2 mmol) was dissolved by heating in 20 mL of ethanol. To this solution, an ethanolic solution (10 mL) of bis(acetylacetonato)dioxomolybdenum(VI) (0.326 g, 1 mmol) was added. The resulting solution was refluxed for 10–12 h and then concentrated to half of its volume. The resulting precipitate was suction filtered and washed several times using 1:1 ethanol–water and dried *in vacuo*. The analytical data of the complexes are given in Table 3.

2.6. Analyses

Carbon, hydrogen, and nitrogen were determined microanalytically at the Central Drug Research Institute, SAIF, Lucknow. The metal content in each chelate was determined (Maurya et al., 1993) as follows: A weighed amount (~200 mg) of the chelate was first decomposed by heating with concentrated nitric acid and then strongly heating the residue over 800 °C for 1 h until a constant weight was obtained. The residue was weighed as MoO_3.

Table 2 Characterization data of the synthesized oxime derivatives.

S. No.	Ligand(empirical formula) (F.W.)	Analyses, found/(calcd.), %			Color	Decomposition temp. (°C)
		C	H	N		
I	aomppH($C_{12}H_{13}N_3O_2$) (231)	62.22 (62.34)	5.52 (5.63)	18.09 (18.18)	Golden brown	170
II	mppopH($C_{13}H_{15}N_3O_2$) (245)	63.47 (63.67)	6.05 (6.12)	17.10 (17.14)	Pale cream	160
III	buomppH($C_{14}H_{17}N_3O_2$) (259)	64.75 (64.86)	6.48 (6.56)	16.18 (16.22)	Daffodil	165
IV	ibuomppH($C_{14}H_{17}N_3O_2$) (259)	64.70 (64.86)	6.48 (6.56)	16.15 (16.22)	Volcano	140
V	bomppH($C_{17}H_{15}N_3O_2$) (293)	69.50 (69.62)	5.06 (5.12)	14.29 (14.33)	Sugar cane color	155

Table 3 Some important IR spectral bands (cm^{-1}) of the synthesized oxime derivative.

S. No.	Ligands	ν(C═O)(pyrazolone)	ν(C═N)(oxime)	ν(C═N)(pyrazolone)	ν(OH)	ν(N–O)
I	aomppH	1660	1620	1590	3200	1020
II	mppopH	1664	1656	1602	3451	1044
III	bomppH	1685	1620	1590	3040	1020
IV	ibuomppH	1685	1620	1590	3040	1020
V	bomppH	1675	1610	1590	3080	1010

2.7. Physical methods

Electronic spectra of the complexes were recorded in dimethylformamide on an ATI Unicam UV-2–100 UV/visible spectrophotometer in our Department. ^{1}H NMR spectra of compounds were recorded in DMSO-d_6 at Central Drug. Research Institute, SAIF, Lucknow. The solid-state infrared spectra were recorded in KBr pellets using Perkin–Elmer model 1620 FT-IR spectrophotometer at the Indian Institute of Technology, Roorkee and also on FT-IR 8400S SHIMADZU at our own Department. Conductance measurements were done at room temperature in dimethylformamide using a Toshniwal Conductivity Bridge and dip type cell with a smooth platinum electrode of cell constant 1.02. Decomposition temperatures of the oxime derivatives and chelates were recorded using an electrothermal apparatus having the capacity to record temperature up to 360 °C. Thermogravimetric analyses of the samples were done at SAIF, Indian Institute of Technology, Mumbai. Mass spectra were recorded at Sophisticated Analytical Instrumentation Facility, CDRI. Lucknow. Magnetic measurement was performed by the Vibrating Sample Magnetometer method.

2.8. Molecular modeling studies

The 3D molecular modeling of a representative compound was carried out on a CS Chem 3D Ultra Molecular Modeling and Analysis Program (www.cambridgesoft.com). It an interactive graphics program that allows rapid structure building, geometry optimization with minimum energy and molecular display. It has ability to handle transition metal compounds.

3. Results and discussion

3.1. Composition and characterization of the oxime derivatives

The oxime derivatives used in the present investigation were prepared as shown in reaction scheme given in Scheme 2.

The compositions of the ligands are consistent with the micro-analytical data. The IR spectra of these oximino derivatives have a band at 1660–1685 cm^{-1}, which is assigned to ν(C═O) (cyclic) of the pyrazolone skeleton. A strong band at 1610–1656 cm^{-1} in these derivatives is assigned to ν(C═N) (oxime). Another strong band observed in all the oxime derivatives at 1590–1602 cm^{-1} is most probably due to ν(C═N) (cyclic) of the pyrazolone skeleton. All the oxime derivatives show medium/broad bands with fine structure in the range 3040–3451 cm^{-1}, which may be due to ν(OH) of the oxime group. The observed low value of ν(OH) suggests the presence of intramolecular hydrogen bonding in the derivatives. A new band observed at 1010–1044 cm^{-1} in the oxime derivatives, unlike the parent carbonyl compound, may be assigned to ν(N–O). The overall IR results conclude that all the oxime derivatives exist in ketonic form in the solid state as shown in the scheme above.

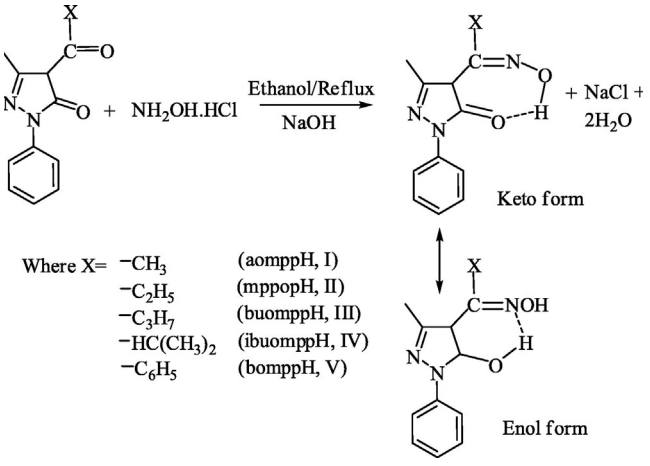

Scheme 2 Synthesis of oxime derivatives.

The proton NMR spectra of two representative ligands namely mppopH (II) (Fig. 4) and buomppH (III) (Fig. 5) were recorded in DMSO-d_6. The proton signals due to aromatic protons of the phenyl ring in the two ligands displayed as multiplets in the region δ 7.194–7.913 and δ 7.173–7.939 ppm,

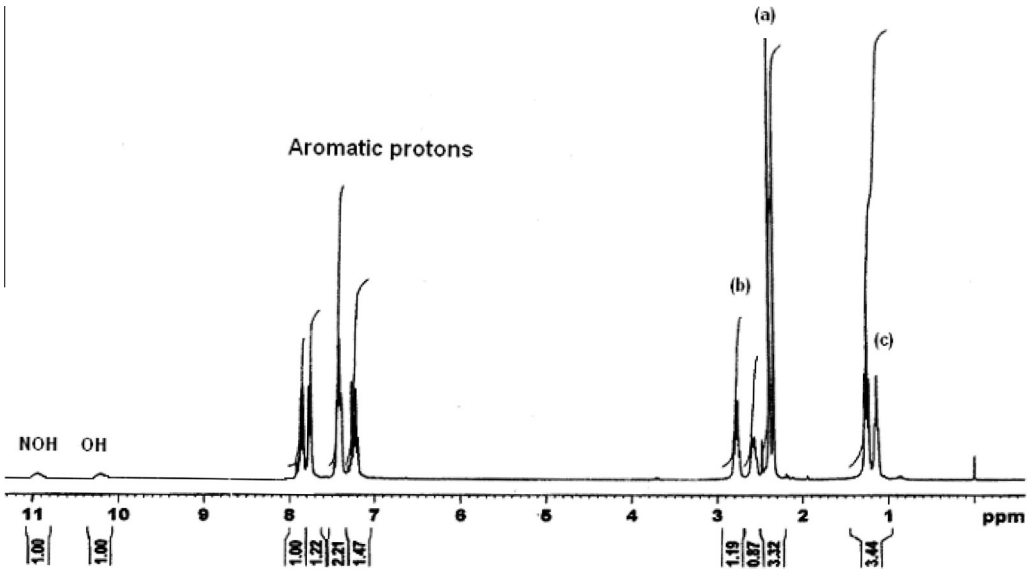

Figure 4 ^{1}H NMR spectrum of mppopH (II).

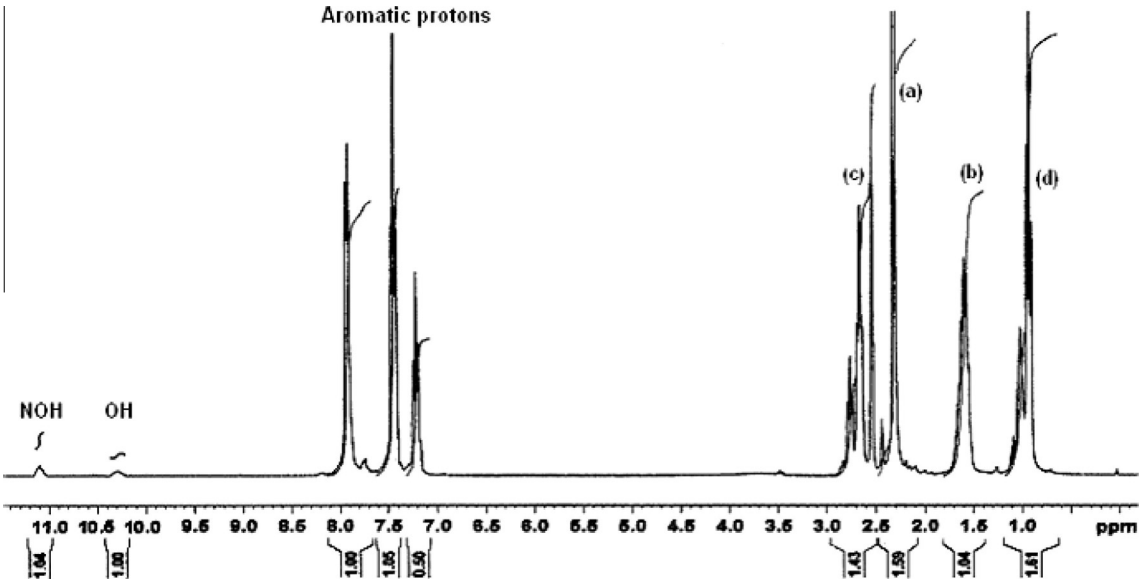

Figure 5 ^{1}H NMR spectrum of buomppH (III).

respectively. The other proton signals in case of ligand (II) at δ 2.740–2.789 (quartet), δ 2.342 (singlet) and at δ 1.051–1.140 (triplet) ppm are most probably due to proton groups, such as $-CH_2$ (**b**), $-CH_3$ (**a**), and $-CH_3$ (**c**), respectively. In case of the ligand (III) proton signals at δ 2.642–2.858 (multiplets), δ 2.317 (singlet), δ 1.576–1.623 (triplet) and δ 0.902–0.927 (triplet) ppm are due to proton groups likely to be $-CH_2$ (**c**), $-CH_3$ (**a**), $-CH_2$ (**b**) and $-CH_3$ (**d**), respectively. Both the ligands displayed two singlet proton signals at δ 10.240–10.422 and δ 10.986–11.101 ppm most probably due to enolic (OH) (cyclic) and –NOH (oxime), respectively. The indexing of various protons is given in Fig. 6.

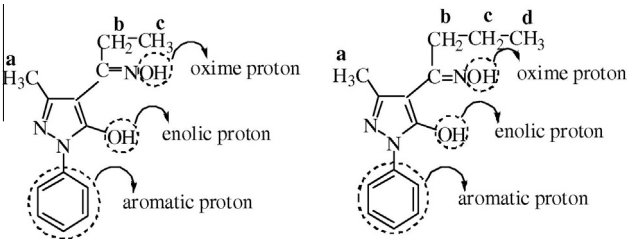

Figure 6 Indexing of various protons in ligands II and III.

The presence of a proton signal at δ 10.240–10.422 ppm suggests that the ligand exist in enolic form in DMSO-d_6 (solvent used for NMR). Contrary to this, all the ligands exist in ketonic form in the solid state as concluded from the IR spectral studies discussed above.

Table 4 Analytical data and some physical properties of the synthesized complexes.

S. No.	Complex*(empirical formula)(F.W.)	Analyses, found/(calcD.),%				Color	Decomp. Temp.(°C)	Yield (%)	Λ_M(ohm^{-1} cm^2 mol^{-1})
		C	H	N	Mo				
1	$[MoO_2(aomppH)_2(H_2O)_2]$ $(C_{24}H_{28}N_6O_8Mo)(623.94)$	46.04 (46.16)	4.29 (4.49)	13.25 (13.46)	15.28 (15.38)	Middle buff	210	50	11.5
2	$[MoO_2(mppopH)_2(H_2O)_2]$ $(C_{26}N_{32}N_6O_8Mo)(651.94)$	47.67 (47.86)	4.82 (4.91)	12.68 (12.88)	14.60 (14.72)	Daffodil	220	60	15.2
3	$[MoO_2(buomppH)_2(H_2O)_2]$ $(C_{28}H_{36}N_6O_8Mo)(679.94)$	49.29 (49.42)	5.15 (5.29)	12.15 (12.35)	14.05 (14.11)	Yellow	240	52	14.1
4	$[MoO_2(ibuomppH)_2(H_2O)_2]$ $(C_{28}H_{36}N_6O_8Mo)(679.94)$	49.30 (49.42)	5.12 (5.29)	12.20 (12.35)	14.02 (14.11)	Deep green	220	50	12.4
5	$[MoO_2(bomppH)_2(H_2O)_2]$ $(C_{34}H_{32}N_6O_8Mo)(747.94)$	54.42 (54.55)	4.20 (4.28)	11.13 (11.23)	12.67 (12.83)	Leaf brown	200	52	10.1

* All the compounds were found to be diamagnetic.

Table 5 Some important IR spectral bands (cm^{-1}) of the synthesized complexes.

S. No.	Complex	$\nu_s(MoO_2)$	$\nu_{as}(MoO_2)$	ν(C–O) (Enolic)	ν(C=N) (oxime)	ν(C=N) (pyrazolone)	ν(OH)	δ(O–H···O)	ν(Mo–O)	ν(Mo–N)	ν(N–O)
1	$[MoO_2(aomppH)_2(H_2O)_2]$	950	910	1126	1578	1612	3401	1724	508	430	1091
2	$[MoO_2(mppopH)_2(H_2O)_2]$	941	913	1167	1578	1605	3437	1659	517	497	1079
3	$[MoO_2(buomppH)_2(H_2O)_2]$	941	913	1227	1567	1605	3430	1658	512	468	1079
4	$[MoO_2(ibuomppH)_2(H_2O)_2]$	991	912	1221	1571	1608	3432	1708	510	456	1091
5	$[MoO_2(bomppH)_2(H_2O)_2]$	951	912	1164	1569	1599	3375	1686	510	450	1073

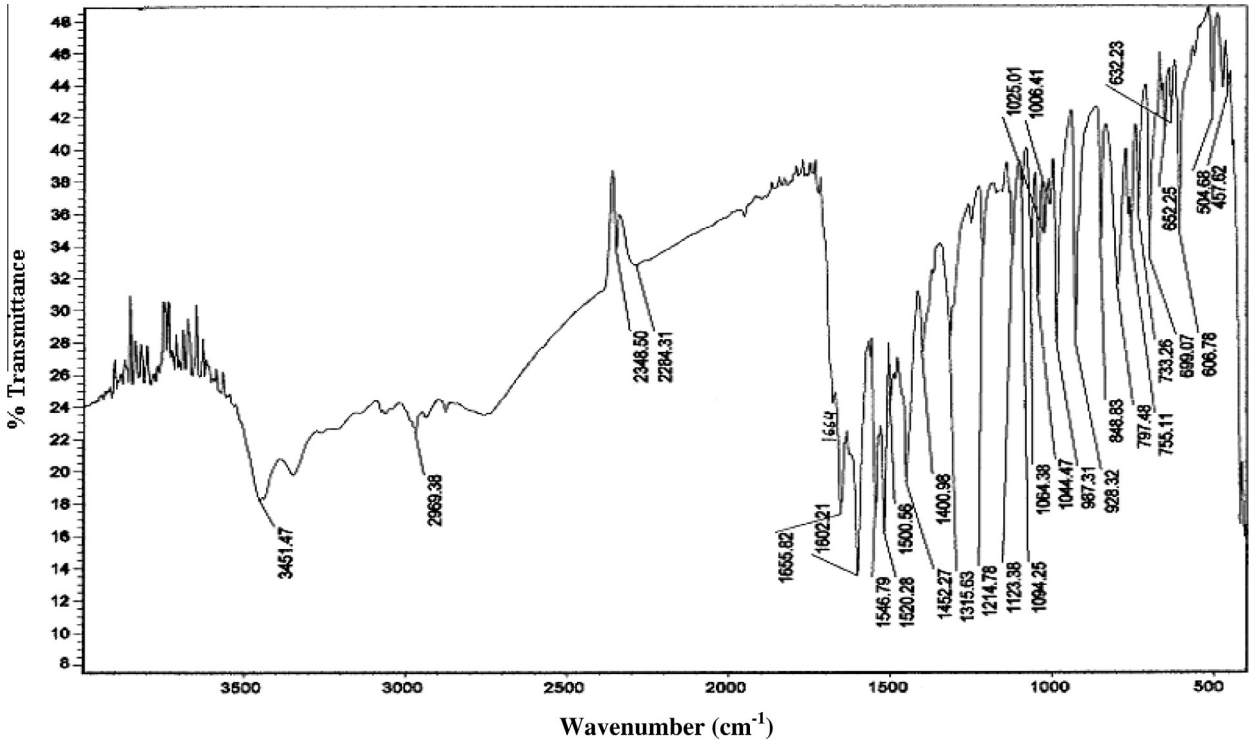

Figure 7 IR spectrum of mppopH (II).

3.2. Characterization of complexes

The formation of metal chelates can be represented by the following general equation:

$$[MoO_2(acac)_2] + 2LH \xrightarrow[\text{Reflux}]{\text{Ethanol (95\%)}} [MoO_2(L)_2(H_2O)] + 2acacH$$

Where LH = aomppH, mppopH, buomppH, ibumppH or bomppH

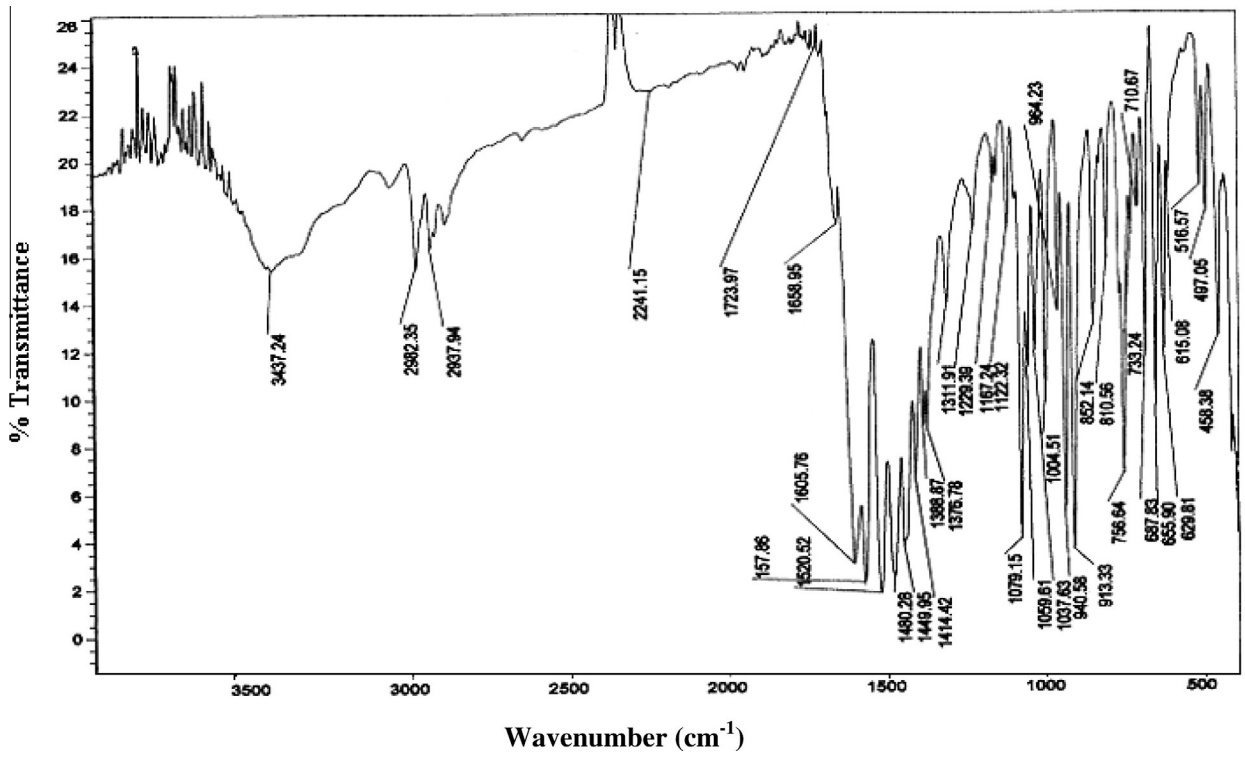

Figure 8 IR spectrum of $[MoO_2(mppopH)_2(H_2O)_2]$ (**2**).

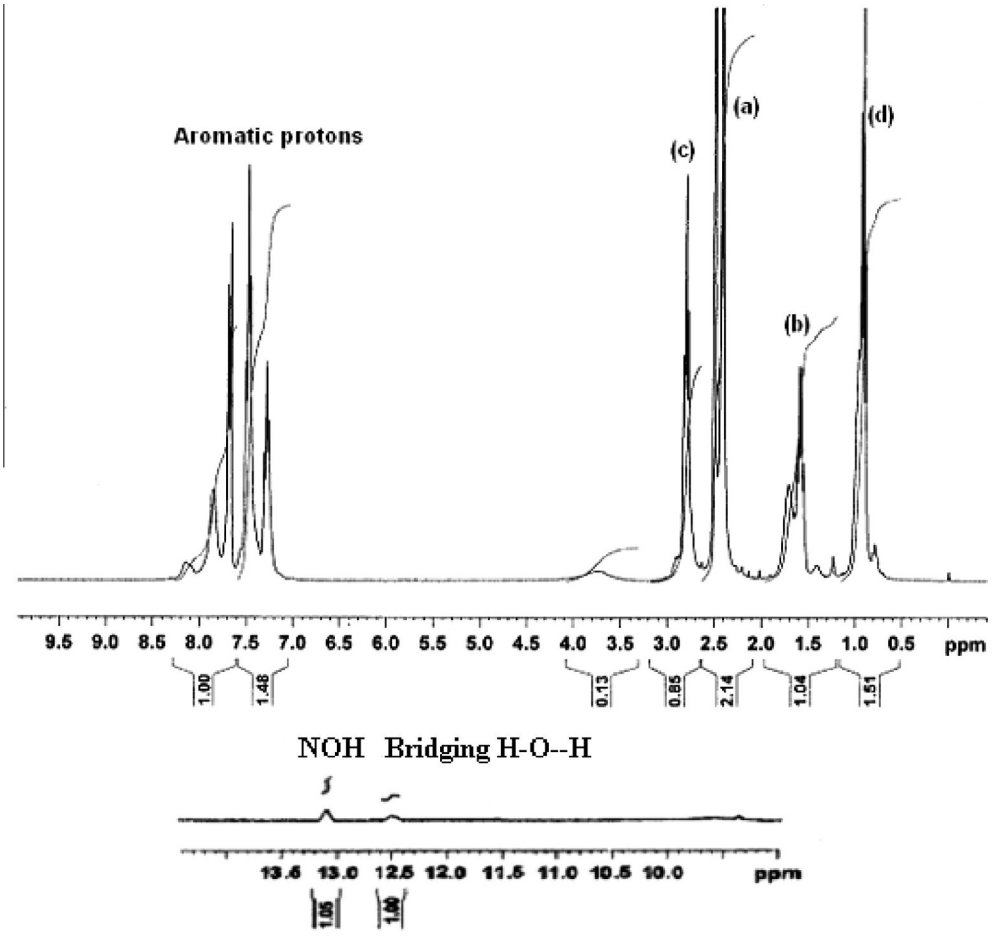

Figure 9 ^{1}HNMR spectrum of $[MoO_2(buomppH)_2(H_2O)_2]$ (**3**).

Table 6 Electronic spectral data of synthesized complexes.

S. No.	Complex	λ_{max} (nm)	ε (liter mol^{-1} cm^{-1})	Peak assignments
1	$[MoO_2(aomppH)_2(H_2O)_2]$	287	3444	Intra-ligand transition
		328	3703	
		337	3777	
		348	3851	
2	$[MoO_2(mppopH)_2(H_2O)_2]$	282	3461	Intra-ligand transition
		307	3500	
		332	3576	
		347	3884	
		355	3730	
		444	1269	LMCT
3	$[MoO_2(buomppH)_2(H_2O)_2]$	296	3513	Intra-ligand transition
		335	4054	
		357	4432	
4	$[MoO_2(ibuomppH)_2(H_2O)_2]$	269	1105	Intra-ligand transition
		443	194	LMCT
5	$[MoO_2(bomppH)_2(H_2O)_2]$	293	3642	Intra-ligand transition
		340	3607	
		352	3714	

The driving force for the reaction in order to form these chelates along with the elimination of two molecules of acetylacetone (acacH) is the better donating (Maurya et al., 2003c) capability of the oxime derivatives compared to acetylacetone anion.

The synthesized complexes are colored, non-hygroscopic and air stable solids. They are thermally stable and their decomposition temperatures are given in the Table 4. These are soluble in dimethylformamide and dimethylsulfoxide, and insoluble in all other common organic solvents. Some physical properties of the complexes are also given in Table 4. The formulations of these complexes are based on their elemental analyses, infrared spectra, magnetic measurements, NMR, mass, thermogravimetry, and electronic spectral studies.

3.3. IR spectral studies

The MoO_2^{2+} moiety prefers to form a *cis*-dioxo grouping due to the maximum utilization of the *d*-orbital for bonding. The dioxo-configuration is characterized by two infrared active modes of ν_s(O═Mo═O) and ν_{as}(O═Mo═O) in C_{2V} symmetry. The *trans*-MoO_2^{2+} moiety would exhibit a single infrared active stretching band of ν_{as}(O═Mo═O). The presence of two infrared bands in the 910–913 and 941–991 cm^{-1} regions due to ν_{as}(O═Mo═O) and ν_s(O═Mo═O), respectively, in the present complexes is strongly indicative of the *cis*-MoO_2^{2+} structures (Syamal and Maurya, 1989; Maurya et al., 1995a).

The coordination of oxime nitrogen is inferred by a shift to lower frequencies[57] (Maurya et al., 2003d) in the ν(C═N) (Oxime) (1567–1578 cm^{-1}) in all the complexes as compared to that of the free oxime derivatives at 1610–1656 cm^{-1}. This is further supported by shifting of the ν(N–O) to a higher wave number (1073–1091 cm^{-1}) (Yildim et al., 2003; Maurya et al., 2003d; Karatas et al., 1991c) in the complexes as compared to that of the free oxime derivatives appearing at 1010–1044 cm^{-1}. All the oxime derivatives display a band in the region of 1590–1602 cm^{-1}, which may be due to ν(C═N^2) (pyrazoline

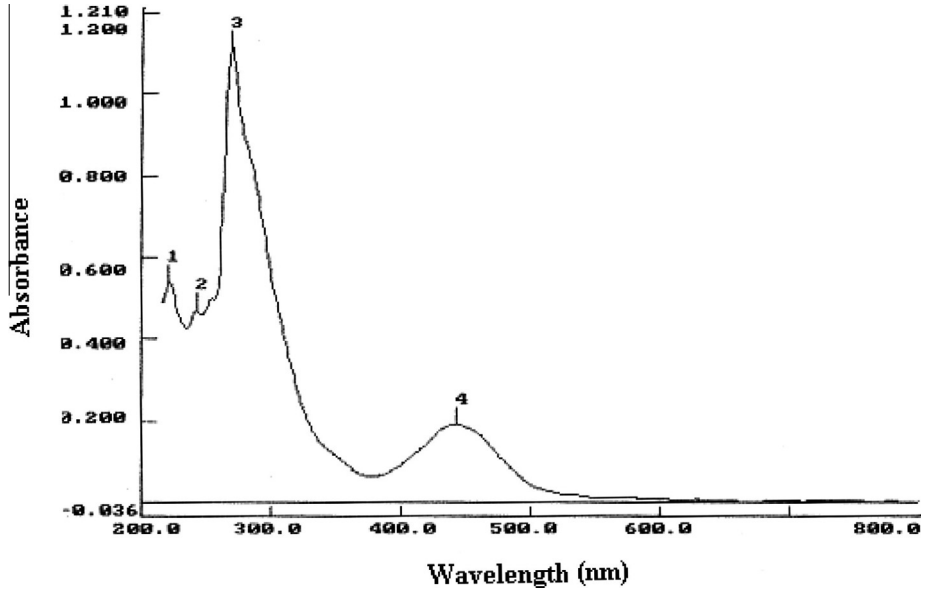

Figure 10 Electronic spectrum of $[MoO_2(ibuomppH)_2(H_2O)_2]$ (**4**).

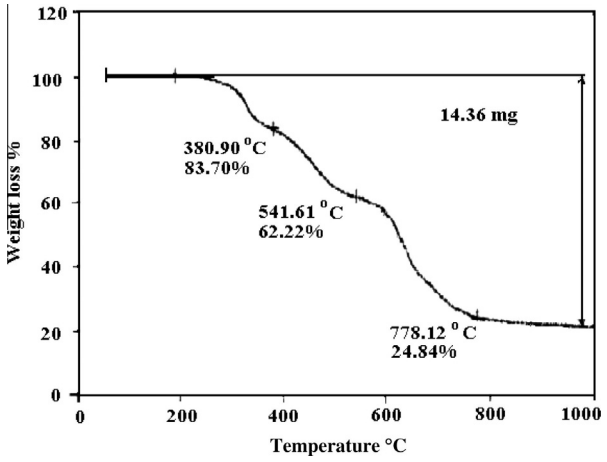

Figure 11 TG curve of $[MoO_2(mppopH)_2(H_2O)_2]$ (**2**).

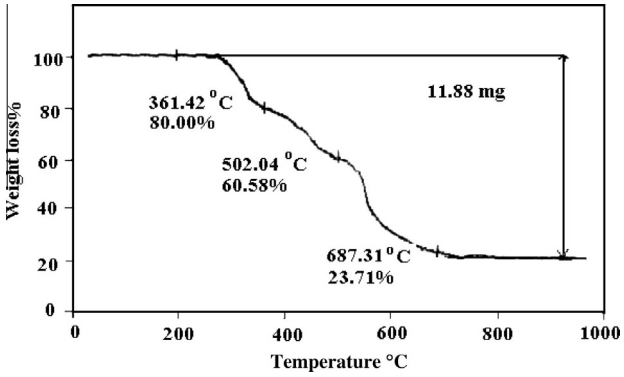

Figure 12 TG curve of $[MoO_2(buomppH)_2(H_2O)_2]$ (**3**).

ring). This band remains almost unchanged in all the metal chelates. This indicates that the ring nitrogen N^2 does not take part in coordination, which is in agreement to our previous observation (Maurya et al., 2003b). The absence of a strong band at 1660–1685 cm^{-1} due to ν(C═O) and the appearance of a new band in the region of 1126–1227 cm^{-1} assignable to ν(C–O) (enolic), may be taken as diagnostic of coordination of cyclic oxygen to the metal center in the enol form (Kharodawala and Rana, 2003; Maurya et al., 2007) after deprotonation. The coordination of oxime nitrogen and cyclic oxygen is further supported by the appearance of two non-ligand bands at 508–517 and 430–497 cm^{-1} assignable to ν(M–O) and ν(M–N), respectively (Maurya et al., 2003a).

The IR spectra of all the complexes show a broad band centered at 3375–3437 cm^{-1}. This suggests the presence of coordinated water molecules. A weak band at 1658–1724 cm^{-1} in the IR spectra of all the complexes can be ascribed to the intermolecular hydrogen bonded O–H···O (between oxime OH group and coordinated water oxygen) bending vibration (Chakravorty, 1974). The important infrared spectral bands of the oxime derivatives and complexes in the present investigation are given in Tables 3 and 5, respectively. The IR spectra of the ligand, mppopH (II), and its complex $[MoO_2(mppopH)_2(H_2O)_2]$ (**2**) are given in Figs. 7 and 8, respectively.

3.4. ^1H NMR spectral studies

The ^1H NMR spectrum of a representative compound $[MoO_2(buomppH)_2(H_2O)_2]$ (**3**) (Fig. 9) was recorded in DMSO-d_6 to compare its result with the respective ligand. The absence of an enolic proton (cyclic) signal at δ 10.422 in the ligand was found to be absent in the spectrum of this complex. This shows the coordination of enolic oxygen after deprotonation to the metal center in this complex. This is in agreement with the IR spectral results related to the coordina-

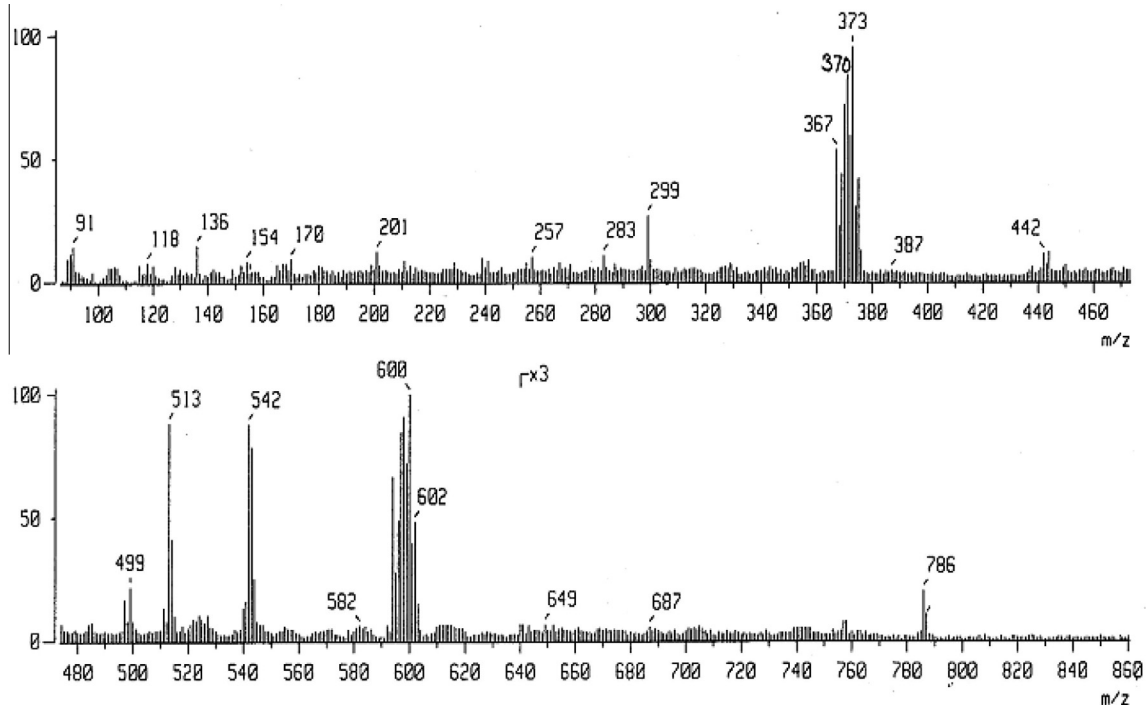

Figure 13 Mass spectrum of $[MoO_2(buomppH)_2(H_2O)_2]$ (**3**).

tion of ligands under discussion. Other proton signals in the complex are δ 2.424 (singlet) $-CH_3$ (**a**), δ 1.577–1.625 (triplet) $-CH_2$ (**b**), δ 2.595–2.912 (multiplets) $-CH_2$ (**c**), δ 0.916–0.969 (triplet) $-CH_3$ (**d**) and δ 7.268–8.144 (multiples) (aromatic protons).

Two more proton signals were observed at δ 12.501 and δ 13.173 ppm in this complex, which are most probably due to protons of hydrogen bonded coordinated water molecules, and hydrogen bonded oxime proton (Zulfikaroglu et al., 2003), respectively.

3.5. Electronic spectral studies

Electronic spectra of all the complexes were recorded in 10^{-3} M in dimethylformamide solutions. The electronic spectral peaks observed in each of the complexes along with their molar extinction coefficient are given in Table 6. The high intensity spectral peak in UV-region in each of the complexes is due to intra-ligand transition. A medium to weak intensity peak near 443–444 nm in complexes (**2**) and (**4**) may be due to the ligand to metal charge transfer transitions (LMCT). The nonappearance of the LMCT band in the other three complexes is most probably due to its poor intensity. The electronic spectrum of $[MoO_2(ibuomppH)_2(H_2O)_2]$ (**4**) is given in Fig. 10.

3.6. Thermogravimetric studies

The thermogravimetric curves of two representative compounds $[MoO_2(mppopH)_2(H_2O)_2]$ (**2**) (Fig. 11) $[MoO_2(buomppH)_2(H_2O)_2]$ (**3**) (Fig. 12) were recorded in the temperature range of 25–1000 °C at the heating rate of 15 °C per minute. The compound (**2**) shows a weight loss of 5.3% at 300 °C with start of weight loss at 240 °C, corresponding to the elimination of two moles of coordinated water (calcd. weight loss for two mole H_2O = 5.52%). It shows a second weight loss of 42.2% at 587 °C corresponding to the elimination of one coordinated oxime ligand group (calcd. weight loss of one oxime ligand group = 42.94%). The final weight loss (obs. = 80.0%) at 778.12 °C corresponds to the elimination of one mole oxime ligand group (calcd. weight loss = 80.37%). The final residue at ~780 °C (obs. = 20.0%) corresponds to MoO_3 (calcd. = 22.07%).

Similar to compound (**2**), the compound (**3**) displayed the following three weight losses:

S. No.	% wt. loss (obs.)	% wt. loss (calcd.)	Elimination of	at (°C)
1	5.3	5.29	Two coordinated water molecules	300
2	43.5	43.23	One ligand group	520
3	80.0	81.16	One ligand group	725

The final residue at ~780 °C (obs. = 21.0%) corresponds to MoO_3 (calcd. = 21.03%). As the MoO_3 is known to volatilize above 800 °C (melting point 795 °C (Greenwood and Earnshaw, 1984) and loose the weight, the TG plots will never be flat if these were reordered up to 1000 °C. Hence, both the TG plots appeared to be effectively recorded up to 800 °C, and so these are flat after ca. 750 °C.

3.7. Mass spectral studies

The FAB mass spectrum of a representative compound $[MoO_2(buomppH)_2(H_2O)]$ (**3**) (Fig. 13) is recorded on a JEOL SX 102/DA-6000 Mass Spectrometer/Data system using ar-

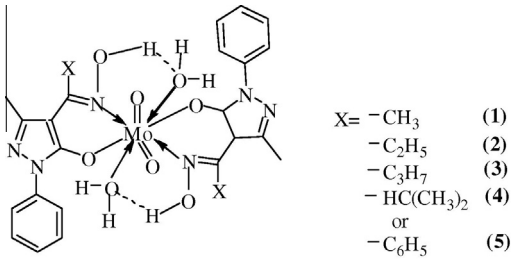

Figure 15 Proposed structure of complexes.

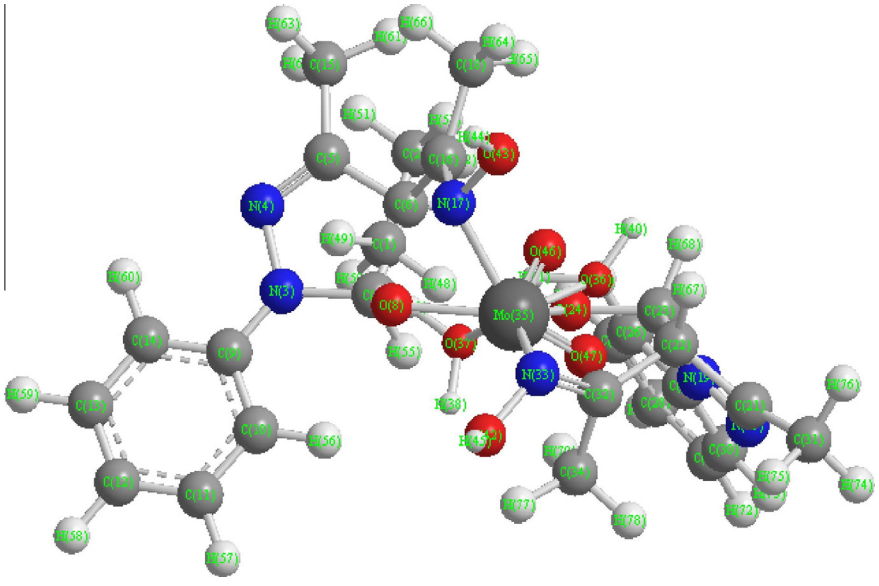

Figure 14 3D structure of compound (**1**).

Table 7 Various bond lengths of compound $[MoO_2(aomppH)_2(H_2O)_2]$ (**1**).

S. No.	Atoms	Actual bond length	Optimal bond length	S. No.	Atoms	Actual bond length	Optimal bond length
1	C(2)–H(53)	1.113	1.113	43	C(22)–C(32)	1.497	1.497
2	C(2)–H(52)	1.113	1.113	44	C(22)–C(23)	1.523	1.514
3	C(2)–H(51)	1.113	1.113	45	C(21)–C(31)	1.497	1.497
4	C(1)–H(50)	1.113	1.113	45	C(21)–C(22)	1.497	1.497
5	C(1)–H(49)	1.113	1.113	47	N(20)–C(21)	1.4988	1.26
6	C(1)–H(48)	1.113	1.113	48	N(19)–C(25)	1.266	1.462
7	C(1)–C(2)	1.523	1.523	49	N(19)–C(23)	1.47	1.47
8	O(43)–H(44)	0.942	0.942	50	N(19)–N(20)	1.23	1.426
9	O(42)–H(45)	0.942	0.942	51	C(18)–H(66)	1.113	1.113
10	O(37)–H(39)	0.986	–	52	C(18)–H(65)	1.113	1.113
11	O(37)–H(38)	0.986	–	53	C(18)–H(64)	1.113	1.113
12	O(36)–H(41)	0.986	–	54	N(17)–Mo(35)	1.9741	–
13	O(36)–H(40)	0.986	–	55	N(17)–O(43)	1.316	–
13	Mo(35)–O(47)	1.5353	–	56	C(16)–C(18)	1.497	1.497
15	Mo(35)–O(46)	1.8428	–	57	C(16)–N(17)	1.377	1.377
16	O(36)–Mo(35)	1.8488	–	58	C(15)—H(63)	1.113	1.113
17	Mo(35)–O(37)	1.5202	–	59	C(15)–H(62)	1.113	1.113
18	C(34)–H(79)	1.113	1.113	60	C(15)–H(61)	1.113	1.113
19	C(34)–H(78)	1.113	1.113	61	C(14)–H(60)	1.1	1.1
20	C(34)–H(77)	1.113	1.113	62	C(13)–H(59)	1.1	1.1
21	N(33)–O(42)	1.316	–	63	C(13)–C(14)	1.337	1.42
22	N(33)–Mo(35)	1.976	–	64	C(12)–H(58)	1.1	1.1
23	C(32)–C(34)	1.497	1.497	65	C(12)–C(13)	1.337	1.42
24	C(32)–N(33)	1.6947	1.377	66	C(11)–H(57)	1.1	1.1
25	C(31)–H(76)	1.113	1.113	67	C(11)–C(12)	1.337	1.42
26	C(31)–H(75)	1.113	1.113	68	C(10)–H(56)	1.1	1.1
27	C(31)–H(74)	1.113	1.113	69	C(10)–C(11)	1.337	1.42
28	C(30)–H(73)	1.1	1.1	70	C(9)–C(14)	1.337	1.42
29	C(29)–H(72)	1.1	1.1	71	C(9)–C(10)	1.337	1.42
30	C(29)–C(30)	1.337	1.42	72	O(8)–Mo(35)	1.94	–
31	C(28)–H(71)	1.1	1.1	73	C(7)–H(55)	1.113	1.111
32	C(28)–C(29)	1.337	1.42	74	C(7)–O(8)	1.402	1.391
33	C(27)–H(70)	1.1	1.1	75	C(6)–H(54)	1.113	1.113
34	C(27)–C(28)	1.337	1.42	76	C(6)–C(16)	1.497	1.497
35	C(26)–H(69)	1.1	1.1	77	C(6)–C(7)	1.523	1.514
36	C(26)–C(27)	1.337	1.42	78	C(5)–C(15)	1.497	1.497
37	C(25)–C(30)	1.337	1.42	79	C(5)–C(6)	1.497	1.497
38	C(25)–C(26)	1.337	1.42	80	N(4)–C(5)	1.26	1.26
39	O(24)–Mo(35)	1.94	–	81	N(3)–C(9)	1.266	1.462
40	C(23)–H(68)	1.113	1.111	82	N(3)–C(7)	1.47	1.47
41	C(23)–O(24)	1.402	1.391	83	N(3)–N(4)	1.4219	1.426
42	C(22)–H(67)	1.113	1.113				

gon/xenon (6 KV, 10 mA) as the FAB gas. The accelerating voltage was 10 KV and the spectrum was recorded at room temperature. *m*-Nitrobenzyl alcohol (NBA) was used as the matrix. The matrix peaks were supposed to appear at *m*/*z* 136, 137, 154, 289, 307 in the absence of any metal ion. If metal ions are present, these peaks may be shifted accordingly.

The mass spectral peaks observed at 136 and 154 *m*/*z* are matrix peaks. The spectral peak observed at 257, 513, 370, 387, 600, and 542 *m*/*z* are most probably due to the following types of ion associations:

(i) $[buomppH]^+$ (258) $- H^+ = 257$
(ii) $[buomppH]^+$ (258) + $(Mo = O)^+$ (111.94) = 370
(iii) $[buomppH]^+$ (258) + $[O{=}Mo{=}O]^+$ (127.94) + H^+ = 387
(iv) $2[buomppH]^+$ (516) $- 3H^+ = 513$
(v) $[Base\ peak]^+$ (600) $- {}^*[C_3H_7]^+$ (43) $- {}^*[CH_3]^+$ (15) = 542
(vi) $[Molecular\ ion]^+$ (643.94) $- {}^*[C_3H_7]^+$ (43) = 600 (Base peak)

*From butyryl oxime

These results are consistent with the proposed molecular composition of the complex (**3**).

3.8. Conductance measurements

The molar conductivities of all the complexes in 10^{-3}M DMF solution are in the range 10.1–15.2 $ohm^{-1}\ cm^2\ mol^{-1}$ (Table 4) as expected for non-electrolytes (Geary, 1971). Such a non-zero molar conductance value for each of the complexes in the present study is most probably due to the strong donor

Table 8 Various bond angles of compound $[MoO_2(aomppH)_2(H_2O)_2]$ (**1**).

S. No.	Atoms	Actual bond angles	Optimal bond angles	S. No.	Atoms	Actual bond angles	Optimal bond angles
1	H(53)–C(2)–H(52)	109.5199	109	81	O(47)–Mo(35)–O(24)	36.6947	–
2	H(53)–C(2)–H(51)	109.4619	109	82	O(47)–Mo(35)–N(17)	142.7106	–
3	H(53)–C(2)–C(1)	109.4615	110	83	O(47)–Mo(35)–O(8)	133.1707	–
4	H(52)–C(2)–H(51)	109.4419	109	84	O(46)–Mo(35)–O(37)	70.4451	–
5	H(52)–C(2)–C(1)	109.4416	110	85	O(46)–Mo(35)–O(36)	29.6984	–
6	H(51)–C(2)–C(1)	109.5005	110	86	O(46)–Mo(35)–N(33)	153.3882	–
7	H(50)–C(1)–H(49)	109.5198	109	87	O(46)–Mo(35)–O(24)	30.6141	–
8	H(50)–C(1)–H(48)	109.4619	109	88	O(46)–Mo(35)–N(17)	79.0453	–
9	H(50)–C(1)–C(2)	109.4617	110	89	O(46)–Mo(35)–O(8)	96.5432	–
10	H(49)–C(1)–H(48)	109.442	109	90	O(37)–Mo(35)–O(36)	87.443	–
11	H(49)–C(1)–C(2)	109.4416	110	91	O(37)–Mo(35)–N(33)	131.1412	–
12	H(48)–C(1)–C(2)	109.5003	110	92	O(37)–Mo(35)–O(24)	65.2425	–
13	H(72)–C(29)–C(30)	119.9998	120	93	O(37)–Mo(35)–N(17)	95.5127	–
13	H(72)–C(29)–C(28)	119.9997	120	94	O(37)–Mo(35)–O(8)	50.2039	–
15	C(30)–C(29)–C(28)	120.0004	–	95	O(36)–Mo(35)–N(33)	125.2943	–
16	H(71)–C(28)–C(29)	120.0002	120	96	O(36)–Mo(35)–O(24)	23.4196	–
17	H(71)–C(28)–C(27)	120.0002	120	97	O(36)–Mo(35)–N(17)	101.4075	–
18	C(29)–C(28)–C(27)	119.9996	–	98	O(36)–Mo(35)–O(8)	125.1198	–
19	H(70)–C(27)–C(28)	119.9996	120	99	N(33)–Mo(35)–O(24)	134.9523	–
20	H(70)–C(27)–C(26)	120.0003	120	100	N(33)–Mo(35)–N(17)	109.4999	–
21	C(28)–C(27)–C(26)	120.0001	–	101	N(33)–Mo(35)–O(8)	109.4999	–
22	H(73)–C(30)–C(29)	120	120	102	O(24)–Mo(35)–N(17)	109.5001	–
23	H(73)–C(30)–C(25)	120.0005	120	103	O(24)–Mo(35)–O(8)	109.4999	–
24	C(29)–C(30)–C(25)	119.9995	–	104	N(17)–Mo(35)–O(8)	58.7561	–
25	H(69)–C(26)–C(27)	120.0001	120	105	H(66)–C(18)–H(65)	109.5196	109
26	H(69)–C(26)–C(25)	119.9997	120	106	H(66)–C(18)–H(64)	109.4624	109
27	C(27)–C(26)–C(25)	120.0003	–	107	H(66)–C(18)–C(16)	109.4617	110
28	C(30)–C(25)–C(26)	120.0001	120	108	H(65)–C(18)–H(64)	109.4421	109
29	C(30)–C(25)–N(19)	119.9998	120	109	H(65)–C(18)–C(16)	109.4418	110
30	C(26)–C(25)–N(19)	120.0001	120	110	H(64)–C(18)–C(16)	109.4998	110
31	H(76)–C(31)–H(75)	109.5202	109	111	O(43)–N(17)–Mo(35)	109.5273	–
32	H(76)–C(31)–H(74)	109.4624	109	112	O(43)–N(17)–C(16)	109.5273	–
33	H(76)–C(31)–C(21)	109.4617	110	113	Mo(35)–N(17)–C(16)	109.1575	–
34	H(75)–C(31)–H(74)	109.4417	109	114	H(59)–C(13)–C(14)	120.0003	120
35	H(75)–C(31)–C(21)	109.4415	110	115	H(59)–C(13)–C(12)	119.9996	120
36	H(74)–C(31)–C(21)	109.4999	110	116	C(14)–C(13)–C(12)	120	–
37	C(21)–N(20)–N(19)	114.4919	115	117	H(58)–C(12)–C(13)	120.0002	120
38	C(25)–N(19)–C(23)	124.5	108	118	H(58)–C(12)–C(11)	120.0003	120
39	C(25)–N(19)–N(20)	124.4998	124	119	C(13)–C(12)–C(11)	119.9995	
40	C(23)–N(19)–N(20)	111.0002	–	120	H(57)–C(11)–C(12)	119.9995	120
41	H(68)–C(23)–O(24)	108.4689	106.7	121	H(57)–C(11)–C(10)	120	120
42	H(68)–C(23)–C(22)	114.5222	109.39	122	C(12)–C(11)–C(10)	120.0005	–
43	H(68)–C(23)–N(19)	111.7232	107.5	123	H(60)–C(14)–C(13)	119.9999	120
44	O(24)–C(23)–C(22)	107.5002	107.7	124	H(60)–C(14)–C(9)	119.9996	120
45	O(24)–C(23)–N(19)	110.5003	–	125	C(13)–C(14)–C(9)	120.0005	–
46	C(22)–C(23)–N(19)	104	–	126	H(56)–C(10)–C(11)	120.0003	120
47	C(31)–C(21)–C(22)	128.9413	117.2	127	H(56)–C(10)–C(9)	119.9997	120
48	C(31)–C(21)–N(20)	128.941	115.1	128	C(11)–C(10)–C(9)	120	–
49	C(22)–C(21)–N(20)	102.1176	115.1	129	C(18)–C(16)–N(17)	120.0001	120
50	H(79)–C(34)–H(78)	109.5202	109	130	C(18)–C(16)–C(6)	120.0002	117.2
51	H(79)–C(34)–H(77)	109.4617	109	131	N(17)–C(16)–C(6)	119.9997	120
52	H(79)–C(34)–C(32)	109.4617	110	132	Mo(35)–O(8)–C(7)	109.4999	–
53	H(78)–C(34)–H(77)	109.442	109	133	H(55)–C(7)–O(8)	108.4688	106.7
54	H(78)–C(34)–C(32)	109.4417	110	134	H(55)–C(7)–C(6)	114.5224	109.39
55	H(77)–C(34)–C(32)	109.5	110	135	H(55)–C(7)–N(3)	111.7237	107.5
56	H(67)–C(22)–C(32)	107.8496	109.39	136	O(8)–C(7)–C(6)	107.5	107.7
57	H(67)–C(22)–C(23)	112.9886	109.39	137	O(8)–C(7)–N(3)	110.4999	–
58	H(67)–C(22)–C(21)	112.9885	109.39	137	C(6)–C(7)–N(3)	103.9999	–
59	C(32)–C(22)–C(23)	109.47	109.51	139	C(14)–C(9)–C(10)	119.9995	120
60	C(32)–C(22)–C(21)	109.4699	109.51	140	C(14)–C(9)–N(3)	120.0006	120
61	C(23)–C(22)–C(21)	104.0001	109.51	141	C(10)–C(9)–N(3)	120	120
62	H(45)–O(42)–N(33)	120.0002		142	H(63)–C(15)–H(62)	109.5198	109
63	C(34)–C(32)–N(33)	115.4565	120	143	H(63)–C(15)–H(61)	109.4621	109
64	C(34)–C(32)–C(22)	115.4567	117.2	144	H(63)–C(15)–C(5)	109.4618	110
65	N(33)–C(32)–C(22)	129.0868	120	145	H(62)–C(15)–H(61)	109.4423	109

Table 8 (*continued*)

S. No.	Atoms	Actual bond angles	Optimal bond angles	S. No.	Atoms	Actual bond angles	Optimal bond angles
66	H(39)–O(37)–H(38)	120.0001	–	146	H(62)–C(15)–C(5)	109.4415	110
67	H(39)–O(37)–Mo(35)	121.5008	–	147	H(61)–C(15)–C(5)	109.4999	110
68	H(38)–O(37)–Mo(35)	95.5876	–	148	H(54)–C(6)–C(16)	107.8498	109.39
69	H(41)–O(36)–H(40)	120.0004	–	149	H(54)–C(6)–C(7)	112.9885	109.39
70	H(41)–O(36)–Mo(35)	55.2093	–	150	H(54)–C(6)–C(5)	112.9885	109.39
71	H(40)–O(36)–Mo(35)	139.3508	–	151	C(16)–C(6)–C(7)	109.4701	109.51
72	O(42)–N(33)–Mo(35)	120.0284	–	152	C(16)–C(6)–C(5)	109.4698	109.51
73	O(42)–N(33)–C(32)	120.0282	–	153	C(7)–C(6)–C(5)	104.0001	109.51
74	Mo(35)–N(33)–C(32)	59.6129	–	154	C(9)–N(3)–C(7)	126.1086	108
75	Mo(35)–O(24)–C(23)	109.5	–	155	C(9)–N(3)–N(4)	126.1079	124
76	H(44)–O(43)–N(17)	120.0002	–	156	C(7)–N(3)–N(4)	107.7834	–
77	O(47)–Mo(35)–O(46)	65.3054	–	157	C(15)–C(5)–C(6)	124.4999	117.2
78	O(47)–Mo(35)–O(37)	83.0583	–	158	C(15)–C(5)–N(4)	124.5001	115.1
79	O(47)–Mo(35)–O(36)	41.3612	–	159	C(6)–C(5)–N(4)	111	115.1
80	O(47)–Mo(35)–N(33)	98.7039	–	160	C(5)–N(4)–N(3)	113.2158	115

capacity of DMF, which may lead to the displacement of the anionic ligand and change of electrolyte type.

3.9. 3D Molecular modeling and analysis

Based on the proposed structures (Fig. 15), the 3D molecular modeling of one of the representative compounds, viz., $[MoO_2(aomppH)_2(H_2O)_2]$ (**1**), was carried out with the CS Chem 3D Ultra Molecular Modeling and Analysis Programme. The details of bond lengths, bond angles as per the 3D structure (Fig. 14) are given in Tables 7 and 8, respectively. For convenience of looking over the different bond lengths and bond angles, the various atoms in the compound in question are numbered in Arabic numerals. In all, 243 measurements of the bond lengths (83 in number), plus the bond angles (160 in number) are listed in the Tables 7 and 8. Except a few cases, optimal values of both the bond lengths and the bond angles are given in the Tables along with the actual ones. The observed bond lengths/bond angles given in the Tables are calculated values as a result of energy optimization in CHEM 3D Ultra [44], while the optimal bond length/optimal bond angle values are the most desirable/favorable (standard) bond lengths/bond angles established by the builder unit of the CHEM 3D. The missing of some values of standard bond lengths/bond angles may be due to the limitations of the software, which we had already noticed in the modeling of other systems (Maurya and Rajput, 2006; Maurya et al., 2008, 2010). In most of the cases, the observed bond lengths and bond angles are close to the optimal values, and thus the proposed structure of compound (**1**) (and also others) is acceptable (Maurya and Rajput, 2006; Maurya et al., 2008, 2010).

4. Conclusions

The satisfactory analytical data and all the physico-chemical studies presented above suggest that the complexes under this investigation may be formulated as $[MoO_2(L)_2(H_2O)_2]$, where LH = 4-acetyloxime-3-methyl-1-phenyl-2-pyrazoline-5-one (aomppH), 3-methyl-1-phenyl-4-propionyloxime-2-pyrazoline-5-one (mppopH), 4-butyryloxime-3-methyl-1-phenyl-2-pyrazoline-5-one (buomppH), 4-isobutyryloxime-3-methyl-1-phenyl-2-pyrazoline-5-one (ibuomppH), 4-benzoyloxime-3-methyl-1-phenyl-2-pyrazoline-5-one (bomppH). Considering the octa-coordination (Maurya et al., 1995b), tentative structures proposed for these complexes are shown in the Fig. 15.

Acknowledgments

The authors are thankful to Professor R.R. Mishra, Vice-Chancellor, Rani Durgavati University, Jabalpur, MP, India, for the encouragement. Analytical facilities provided by the Central Drug Research Institute, Lucknow, India, and the Sophisticated Instrumentation Centre, Indian Institute of Technology, Roorkee and Mumbai are gratefully acknowledged.

References

Abrantes, M., Santos, A.M., Mink, J., Kuhn, F.E., Ramao, C.C., 2003. Organometallics 22, 2112.
Alexandrova, L., D'yachenko, O.G., Kazankov, G.M., Polyakov, V.A., Samuleev, P.V., Sansores, E., Ryabov, A.D., 2000. J. Am. Chem. Soc. 21, 5189.
Banks, C.V., 1963. Analytical Chemistry. Elsevier, Amsterdam.
Brown, D.G., 1973. Prog. Inorg. Chem. 18, 177.
Chakravorty, A., 1974. Coord. Chem. Rev. 13, 1.
Chen, G.J.J., McDonald, J.W., Newton, W.E., 1976. Inorg. Chem. 15, 2612.
Collision, D., Garner, C.D., Joule, J.A., 1996. Chem. Soc. Rev., 25.
Diehl, H. 1940. The Application of the Dioxime to Analytical Chemistry (G. Fredrick Smith Chemical Co., Columbus, Ohio). Van Nostrand, New York.
Elberg, J., Li, G., Gefel, D., Shechter, Y., 1995. Biochemistry 34, 6218.
Enemark, J.H., Cooney, J.J.A., Wang, J.J., Holm, R.H., 2004. Chem. Rev. 104, 1175.
Fillat, C., Rodriguez-Gil, J.E., Guinovart, J.J., 1992. Biochem. J. 282, 659.
Franczek, F.R., Luck, R.L., Wang, G., 2002. Inorg. Chem. Commun. 5, 384.
Geary, W.J., 1971. Coord. Chem. Rev. 7, 81.
Gok, Y., Bekaroglu, O., 1981. Synth. React. Inorg. Met.-Org. Chem. 11, 611.

Goto, Y., Kida, K., Ikeuchi, M., Kaino, Y., Matsuda, H., 1992. Biochem. Pharmacol. 44, 177.
Greenwood, N.N., Earnshaw, A., 1984. Chemistry of the Elements. Pergamon Press, p. 1173.
Gul, A., Bekaroglu, O., 1982. Synth. React. Inorg. Met.-Org. Chem. 12, 889.
Hille, R., 1996. Chem. Rev. 96, 2757.
Irez, G., Bekaroglu, O., 1983. Synth. React. Inorg. Met.-Org. Chem. 13, 781.
Jensen, B.S., 1959. Acta Chem. Scand. 13, 1670.
Karatas, K., Ucan, H.I., 1998. Synth. React. Inorg. Met.-Org. Chem. 28, 383.
Karatas, I., Irez, G., Sezgin, M., 1991a. Synth. React. Inorg. Met.-Org. Chem. 21, 1031.
Karatas, I., Irez, G., Sezgin, M., Ucan, H.I., Beduk, A.D., 1991b. Synth. React. Inorg. Met.-Org. Chem. 21, 1031.
Karatas, I., Irez, G., Sezgin, M., Ucan, H.I., Beduk, D., 1991c. Synth. React. Inorg. Met.-Org. Chem. 21, 1031.
Kharodawala, M.J., Rana, A.K., 2003. Synth. React. Inorg. Met.-Org. Chem. 33, 1483.
Kocak, M., Bekaroglu, O., 1985. Synth. React. Inorg. Met.-Org. Chem. 14, 89.
Kukushkin, V.Y., Pombeiro, A.J.L., 1999. Coord. Chem. Rev. 181, 147.
Li, Y., Fu, X., Gong, B., Zou, X., Tu, X., Chen, J., 2010. J. Mol. Cat. A: Chem. 322, 55.
Masoud, S.M., Ali, G.Y., Youseff, A.R., 1986. Pol. J. Chem. 60, 731–740.
Maurya, R.C., Rajput, S., 2006. J. Mol. Struct. 794, 24.
Maurya, R.C., Mishra, D.D., Rao, N.S., Jayaswal, N.N., Rao, N.N., 1993. Polyhedron 12, 2045.
Maurya, R.C., Mishra, D.D., Rao, N.S., Rao, N.N., 1995a. Synth. React. Inorg. Met.-Org. Chem. 25, 437.
Maurya, R.C., Mishra, D.D., Rao, N.S., Rao, N.N., 1995b. Bull. Chem. Soc., Jpn. 68, 1589.
Maurya, R.C., Patel, P., Rajput, S., 2003a. Synth. React. Inorg. Met.-Org. Chem. 33, 817.
Maurya, R.C., Pillai, V., Rajput, S., 2003b. Synth. React. Inorg. Met.-Org. Chem. 33, 699.
Maurya, R.C., Verma, R., Singh, T., 2003c. Synth. React. Inorg. Met.-Org. Chem. 33, 309.
Maurya, R.C., Verma, R., Sutradhar, D., 2003d. Synth. React. Inorg. Met.-Org. Chem. 33, 435.
Maurya, R.C., Chourasia, J., Martin, M.H., Jhamb, S. 2007. Proceed. Nuclear and Radiochemistry Symposium (NUCAR-2007), Vadodara, India, CA-2, p. 187.
Maurya, R.C., Chourasia, J., Sharma, P., 2008. Indian J. Chem. 47A, 517.
Maurya, R.C., Martin, M.H., Chourasia, J., Sharma, A.K., 2010. Int. J. Curr. Chem. 1, 309.
Mehrotra, R.C., Rai, A.K., Singh, A., Bohra, R., 1975. Inorg. Chim. Acta 13, 91.
Mercimek, B., Pekacar, A.I., Ozcan, E., 1995. Synth. React. Inorg. Met.-Org. Chem. 25, 1571.
Mohanty, R.N., Dash, K.C., 1990. Polyhedron 9, 1011.
Ozcan, E., Mirzaoglu, R., 1988. Synth. React. Inorg. Met.-Org. Chem. 18, 1559.
Ozcelikay, A.T., Baker, D.J., Ingemba, L.N., Pottier, A.M., Henquin, J.C., Brichard, S.M. 1996. Am. J. Physiol., 270 (Endocrinol, Metab. 33), E 344.
Pande, K.C., Patent, U.S., 1966. 3, 352, 672; Chem. Abstr. 1967, 66, 28891C.
Patel, Y.M., Shah, J.R., 1985. Indian J. Chem. 24, 800.
Pekacar, A.I., Ozcan, E., 1994. Macromol. Rep. 31, 651.
Pekacar, A.I., Ozcan, E., 1995a. Macromol. Rep. 32, 1161.
Pekacar, A.I., Ozcan, E., 1995b. Synth. React. Inorg. Met.-Org. Chem. 15, 859.
Reddy, V.K., Reddy, S.M., Reddy, P.R., Reddy, T.S., 2000. Indian J. Chem. Sec. A. 39, 557.
Schrazer, G.M., 1976. Angew. Chem., Int. Ed. 15, 417.
Schrock, R.R., 2004. J. Mol. Catal. A: Chem. 213, 21.
Sevindir, H.C., Mirzaoglu, R., 1992. Synth. React. Inorg. Met.-Org. Chem. 22, 851.
Shah, N.R., Shah, J.H., 1981. J. Indian Chem. Soc. 58, 851.
Shah, N.R., Shah, J.H., 1982a. Indian J. Chem. 21A, 176.
Shah, N.R., Shah, J.H., 1982b. Indian J. Chem. 21A, 312.
Shuter, E. 1995. M. Sc. Thesis University of British Columbia.
Singh, A., Gupta, V.D., Srivastava, G., Mehrotra, R.C., 1974. J. Organomet. Chem. Rev. 64, 145.
Stiefel, E.I., 1979a. Prog. Inorg. Chem. 22, 1.
Stiefel, E.I., 1979b. In: Coughltan, M.P. (Ed.), Molybdenum and Molybdenum-Containing Enzymes. Pergamen Press, Oxford, p. 43.
Syamal, A., Maurya, M.R., 1989. Coord. Chem. Rev. 95, 183.
Tschugaeft, L., 1905. Z. Anorg. Allg. Chem. 46, 144;.
Tschugaeft, L., 1908. Ber. 41, 2219.
Ucan, H.I., Karatas, I., 1991. Synth. React. Inorg. Met.-Org. Chem. 21, 1083.
Ucan, H.I., Mirzaoglu, R., 1990. Synth. React. Inorg. Met.-Org. Chem. 20, 437.
Yildim, S., Pekacar, A.I., Ucan, M., 2003. Synth. React. Inorg. Met.-Org. Chem. 33, 1253.
Zulfikaroglu, A., Tas, M., Bati, H., Bati, B., 2003. Synth. React. Inorg. Met.-Org. Chem. 33, 625.